High-speed degree of polarization imaging with a ferroelectric liquid-crystal modulator

Albéric Jaulin, Laurent Bigue, Pierre Ambs

Optical Engineering 47(3), 033201 (March 2008)

High-speed degree-of-polarization imaging with a ferroelectric liquid-crystal modulator

Albéric Jaulin
Laurent Bigué, MEMBER SPIE
Pierre Ambs, MEMBER SPIE
Université de Haute-Alsace
Ecole Nationale Supérieure d'Ingénieurs Sud Alsace
Laboratoire Modélisation Intelligence Processus Systèmes (EA 2332)
12, rue des Frères Lumière
68093 Mulhouse Cedex, France
E-mail: Alberic.Jaulin@uha.fr

Abstract. Images describing polarimetric characteristics of objects are more and more used when studying complex scenes. In some cases, only the depolarization phenomenon, mostly due to scattering, proves of interest and estimating the degree of polarization (DOP) is sufficient. For a linearly polarized beam under normal incidence, when the materials in the scene exhibit neither birefringence nor dichroism, this comes down to an intensity measurement in two crossed directions. Nevertheless, the classical optical setup, consisting mainly of a rotating polarizer used as a polarization state analyzer, gives good-quality images, but cannot provide dynamic information. In this paper, we propose to use a ferroelectric liquid-crystal modulator in an imaging polarimeter. We demonstrate the use of this modulator as a polarization state analyzer for frame rates up to about 400 Hz. Provided a fast camera is used, we show that the polarimeter allows us to surpass the classical video frame rate. We propose a setup using a rapid CCD camera (up to 233 Hz). Images in DOP are of very high quality and hold their own against images obtained with a classical polarizer. With a faster camera, we were able to obtain images at up to 400 Hz.
[DOI: 10.1117/1.2894811]

Subject terms: polarimetry; imaging system; spatial light modulator; ferroelectric device.

Paper 070489R received Jun. 8, 2007; revised manuscript received Oct. 10, 2007; accepted for publication Nov. 3, 2007; published online Mar. 18, 2008. This paper is a revision of a paper presented at the SPIE conference on Optical Sensing II, April 2006, Strasbourg, France. The paper presented there appears (unrefereed) in SPIE Proceedings Vol. 6576.

1 Introduction

The polarization of light is a physical phenomenon of the highest interest in various domains. Observation of polarization properties of a scene can provide valuable information about the local nature of objects. Therefore, imaging polarization can be used with much benefit in applications such as medical imaging,[1,2] metrology,[3–5] and remote sensing.[6,7] Imaging polarization can be used to study the depolarization due to objects, and then to discriminate materials that would have had the same appearance if polarization had not been taken into account.[8]

Several experimental methods can be used to determine the degree of polarization of a scene. A classical optical setup mainly consists of a rotating polarizer used as a polarization state analyzer. Using liquid-crystal technology, Wolff et al.[9] implemented dynamic measurements using two twisted nematic-liquid-crystal spatial light modulators as polarization rotators. The frame rate obtained with this method is lower than the classical video rate of 50 Hz.

We propose to implement a high-rate imaging system to determine the degree of polarization (DOP). We use a single ferroelectric liquid crystal (FLC) light modulator (able to operate up to 1000 Hz) to obtain two crossed polarization states, and a high-speed camera (either a CMOS camera or a CCD camera). Demonstration of the optical setup is performed with two scenes, one static and the other rotating.

Section 2 deals with the basics of the depolarization phenomenon and the degree of polarization. Section 3 reviews various optical systems used to evaluate the degree of polarization. In Sec. 4, we detail our optical system, which uses a single FLC modulator. Finally, we present some experimental results obtained with our optical setup. In Sec. 5, the image quality is compared with that of the classical setup.

2 Polarization Basics

2.1 *General Definition*

Depolarization can be defined as the transformation of polarized light into unpolarized light and depends on the incident wavelength, illuminated area, and illuminated solid angle.[10] Typical optical elements are usually designed to avoid depolarization. However, most natural and man-made objects produce significant depolarization.[4] For instance, depolarization can be used to compare rough and smooth surfaces.[11] Partial depolarization is observed after light reflection from materials, due to diffusion and/or nonspecular reflection. On paint, metal, and wood surfaces, natural materials, etc., the depolarization is significant, varying from a few percent to 100%.[12] Depolarization can be numerically evaluated by a decrease in the degree of polarization

(DOP).[10] The latter, described in the following, characterizes the randomness of a polarization state.[12]

2.2 *Formalism*

Polarization of a light wave can be fully described by four parameters known as the Stokes polarization parameters or Stokes vector. The first parameter (S_0) is the total intensity of the optical field, and the other three parameters (S_1, S_2, and S_3) describe the polarization state. In a first approach, these parameters can be obtained by six measurements of intensity:

$$\begin{pmatrix} S_0 \\ S_1 \\ S_2 \\ S_3 \end{pmatrix} = \begin{pmatrix} I_0 + I_{90} \\ I_0 - I_{90} \\ I_{45} - I_{-45} \\ I_r - I_l \end{pmatrix}. \quad (1)$$

Here I_0, I_{90}, I_{45}, I_{-45}, I_r, and I_l are respectively the intensity of light with vertical polarization, horizontal polarization, polarization at a 45-deg angle, polarization at a −45-deg angle, right circular polarization, and left circular polarization.

The Stokes parameters are observable real quantities associated with the polarization state of light: S_1 describes linear polarization states compared with reference to a laboratory axis, S_2 describes polarization states at 45 deg to that axis, and S_3 describes the circular component.[13] For a completely polarized beam, a relation between the four Stokes parameters is given by

$$S_0^2 = S_1^2 + S_2^2 + S_3^2. \quad (2)$$

For a totally unpolarized beam, S_1, S_2 and S_3 are zero. For a partially polarized beam, the relation given by Eq. (2) is still valid when the amplitudes and phases fluctuate slowly over very short time intervals, and in general the Stokes parameters satisfy the relation[13]

$$S_0^2 > S_1^2 + S_2^2 + S_3^2. \quad (3)$$

In order to quantify partial polarization, the *degree of polarization* is used.[13] It can be defined as

$$\mathrm{DOP} = \frac{I_{\mathrm{Pol}}}{I_{\mathrm{Tot}}} = \frac{(S_1^2 + S_2^2 + S_3^2)^{1/2}}{S_0}. \quad (4)$$

For a linearly polarized beam under normal incidence, when the materials in the scene do not exhibit birefringence or dichroism, estimating the DOP consists in calculating the partial degree of linear polarization. This operation only requires an intensity measurement in two crossed polarization directions,[14] because in this particular case, the Stokes parameters S_2 and S_3 are zero. Therefore, in this case the expression for the classical DOP can be simplified to[15–17]

$$\mathrm{DOP} = \frac{S_1}{S_0}, \quad (5)$$

$$S_0 = I_0 + I_{90}, \qquad S_1 = I_0 - I_{90}, \quad (6)$$

(a) (b) (c)

Fig. 1 (a) Image with linear polarization parallel to incident polarization, I_0; (b) image with linear polarization perpendicular to incident polarization, I_{90}; (c) DOP image.

$$\mathrm{DOP} = \frac{I_0 - I_{90}}{I_0 + I_{90}}. \quad (7)$$

An image based on this DOP may be referred to as an orthogonal state contrast image (OSCI).[18,19]

2.3 *Considerations About the Degree of Polarization*

Linear DOP evaluation can be used to compare and classify rough and smooth surfaces with a polarization signature.[3] The DOP image also permits one to distinguish between metallic and scattering materials[14] and between different painted surfaces.[20]

The DOP has values between zero and one and provides a summary of the object's depolarizing ability in a single figure. The DOP is zero if the reflected beam is totally unpolarized, and is one if the beam is totally polarized. For the optical setups described in this paper, the DOP depends on emergent polarization states for incident light with linear vertical polarization.[10] For imaging analysis, the DOP is calculated for each pixel of the image after acquisition of two images of crossed polarized intensities. Figure 1 illustrates the imaging calculation of the DOP on a sample including a metallic coin and a piece of polystyrene, illuminated by a linearly polarized monochromatic red He-Ne laser beam. We verify on the DOP image [Fig. 1(c)] that the metallic coin does not depolarize, but that the piece of polystyrene depolarizes strongly.

2.4 *Optical Static Principles for Evaluating the DOP*

In this subsection and the following one, we briefly recall the basic principles of DOP evaluation.

2.4.1 *One single arm with a rotating polarizer and a camera*

The scene is illuminated by a linearly polarized beam. After reflection on the scene, two successive views with crossed linear polarization are acquired by a camera equipped with a rotating polarizer (Fig. 2). The rotating polarizer is given successively two rotation angles.[21] This setup does not allow the user to observe a polarimetric scene at video rate

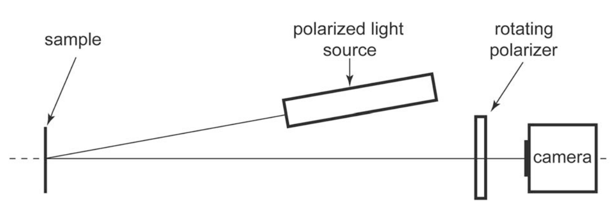

Fig. 2 Optical setup with a rotating polarizer.

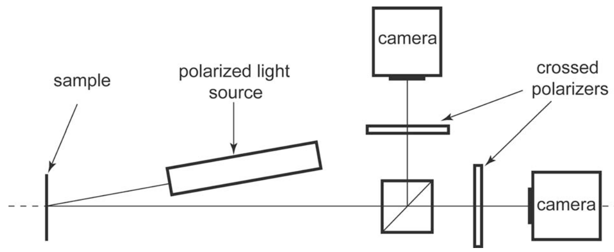

Fig. 3 Optical setup with two fixed polarizers and two cameras.

(50 Hz). Even a motorized mechanical rotation of the polarizer does not permit reaching a video frame rate.

2.4.2 *Two arms with a polarizer and a camera on each arm*

The previous optical setup has been modified in order to simultaneously provide the information in two crossed polarization directions. For this purpose, one detection arm has been added, in which the polarizer is rotated with its axis perpendicular to the axis of the other polarizer (Fig. 3). This system is limited only by the frame rate of the cameras.[21]

2.5 *Optical Dynamic Principles for Evaluating the DOP*

2.5.1 *Industrial system*

This setup is a modified version of the first setup: the rotating polarizer is now fixed, and two twisted nematic-liquid-crystal modulators are placed in front of the fixed polarizer (Fig. 4). Both modulators are used in binary mode[9] as switchable half-wave plates. Four combinations of polarization directions are possible, since the two modulators have been chosen to have different rotary powers. Because of the limited commutation rate of this twisted nematic liquid crystal (about 10 Hz), the overall frame rate is lower than the classical video rate.

2.5.2 *High-quality systems*

These setups, dedicated to astronomy, use two FLC bistable modulators to obtain Stokes parameters. A first solution is to use two $\lambda/2$ modulators in conjunction with $\lambda/8$ wave plates.[22] An improved solution is to use two modulators with different retardations, e.g., $\lambda/2$ and $3\lambda/4$.[23] Since the four Stokes parameters are evaluated, the DOP can be determined. A major drawback of these systems lies in the fact that they need temperature control of the modulators. The frequency of these setups is about 250 Hz.[23] Since the use of a single FLC bistable modulator only allows the user to evaluate two out of the four Stokes parameters, they require two modulators.

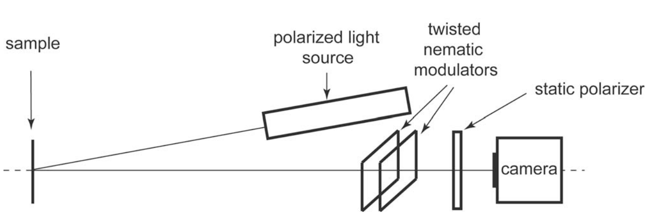

Fig. 4 Optical setup suggested by Wolff et al.[9]

3 Our System with a Ferroelectric-Liquid-Crystal Modulator

We propose a high-quality system simpler than the one just described. We use a single FLC modulator with a standard high-speed camera, without any temperature control.

3.1 *Advantage in Using a Ferroelectric-Liquid-Crystal Modulator*

We aim at designing a single-camera polarimeter able to provide information at a high frame rate, inspired by Wolff's dynamic systems described in Sec. 2.5. The two liquid-crystal modulators are replaced by a single FLC modulator able to run at up to 1000 Hz.[24]

This modulator, manufactured by BNS Inc., acts as a half-wave plate whose axis is continuously tunable from 0 to 45 deg. Unfortunately, this modulator is a half-wave plate only for its design wavelength.[25,26] A FLC cell can be operated at several tens of kilohertz, but this device is pixelated and the electronic addressing scheme limits its frame rate to 1015 Hz.[24,27] FLC cells require one to get a zero time-average voltage, and then, for each image sent to the modulator, the hardware driver sends the inverse image. Consequently, the usable view time is divided by 2. This 512×512-pixel device works in reflection. It has a 15-μm pitch, and each individual pixel can be controlled with eight bits. We fully characterized the device's response for various frame rates.[28] This characteristic can be obtained for each gray level. The study of the variation of amplitude and phase produced by the modulator gives the polarization performance, assuming that the device works as a half-wave plate.

To calculate the DOP, we use only two configurations for each pixel, corresponding to axis orientations of 0 and 45 deg for the half-wave plate. Configurations are obtained with two uniform patterns sent to the FLC modulator. In this particular case, we take advantage of the driving scheme of the FLC modulator. Here, since the 45-deg-axis image corresponds to the 0-deg-axis inverse image, we only need to send one image, which means that the FLC frame rate is not divided by 2.

3.2 *Description of Our Polarimetric Setup*

As an illumination source, we use a 632.8-nm He-Ne laser collimated beam, which is made incoherent thanks to a rotating diffuser, in order to remove speckle (Fig. 5). The incident beam is fully linearly polarized, but the rotating diffuser lowers the initial DOP from 100% to 98%. This beam lights up our test scene in reflection. The test scene is then imaged onto our FLC modulator, and the FLC modulator is imaged onto a camera, through a fixed polarizer. This system does not require any temperature control.

In this configuration, only uniform patterns are displayed on the modulator. We alternatively use two patterns that result in a 45-deg rotation of the liquid-crystal axis. The evaluation comes down to successively analyzing the reflection of the scene with a horizontal and a vertical analyzer. Liquid-crystal devices are known to produce signifi-

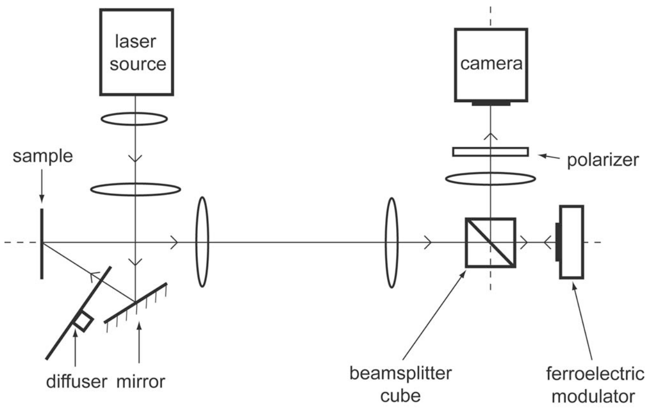

Fig. 5 Optical setup for DOP calculation with a ferroelectric modulator. The extra half-wave plate in front of the modulator is used for adjustment purposes and can be removed.

cant depolarization, but in the present case it is rather limited: An incident fully linearly polarized beam exhibits a DOP of 0.941 after an SLM in the off state, and a DOP of 0.976 after an SLM in the on state.

3.3 *Static Results*

We compared the performance of our dynamic setup with the performance of the classical static setup as described in Sec. 2.4.1. We used a static scene, depicted in Fig. 6, composed of dark pliers holding a one-euro-cent coin lying on a polystyrene chip. A piece of translucent adhesive tape has been placed on the right side of the coin.

We checked that mechanically rotating the polarizer and controlling the modulator to rotate the polarization provide very similar results (the results are acquired with a standard closed-circuit IR (CCIR) analog CCD camera and an 8-bit analog-to-digital conversion card), as reported in Fig. 7.

We chose materials exhibiting various polarization properties. Nevertheless, since we were interested only in observing depolarization, we did not use birefringent or dichroic materials. We can first notice that there is hardly any difference between images produced by the classical polarimeter (with a rotating polarizer) and by our polarimeter with the FLC modulator depolarization. When we analyze the DOP images, as expected, we notice that whereas the coin globally keeps the polarization, the polystyrene chip strongly depolarizes and now clearly appears in gray on a dark background. On the right of the coin, the piece of adhesive tape appears, since it slightly depolarizes.

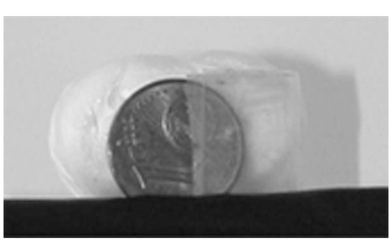

Fig. 6 Static scene used in our tests.

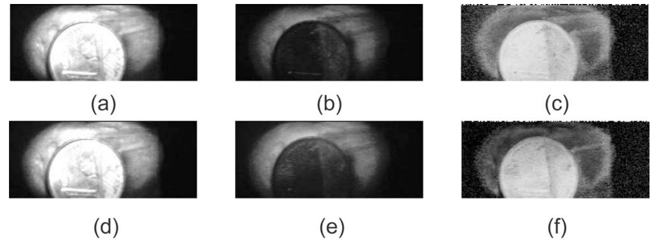

Fig. 7 Images (a) to (c) were acquired with a rotating polarizer; images (d) to (f) were acquired with the ferroelectric modulator. Images (a) and (d) are of the intensity I_0; images (b) and (e) are of the intensity I_{90}; images (c) and (f) are results of DOP calculation.

4 High-Speed Imaging Polarimeter

4.1 *Description of the Dynamic Test Scene*

In order to prove the ability of our device to capture dynamic phenomena, we used a rotating scene (Fig. 8). It is composed of an aluminum plate on which are placed several objects: a polystyrene chip, a one-euro-cent coin that is fixed with a piece of double-sided adhesive tape, and several layers of translucent adhesive tape that have been superimposed.

These various elements modify polarization in various ways, but in this study we are only interested in evaluating depolarization. For instance, we do not consider the fact that the translucent adhesive tape exhibits birefringence in addition to depolarization. We first observed the coin and the double-sided adhesive tape (Table 1, Fig. 9) with a reference polarimeter consisting of a rotating quarter-wave plate and a polarizer. The angular precision for the wave plate can be estimated to 1 deg. These reference measures are compared in the following with those obtained with our liquid-crystal polarimeter.

4.2 *High-Speed Imaging Polarimeter with a CMOS Camera*

The setup is basically the same as the one described in Sec. 3, except that we used a high-speed CMOS camera. This

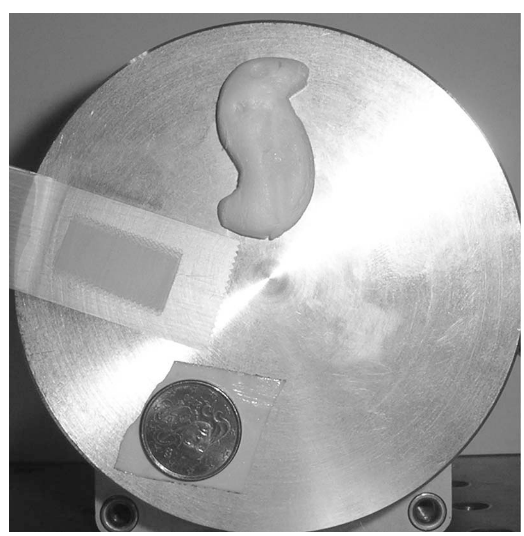

Fig. 8 Rotating scene used in our tests.

Table 1 Polarization properties of the different elements of our dynamic test scene.

	Value		
Quantity	Aluminum wheel	Double-sided adhesive tape	Euro cent coin
S_1	0.836	0.018	0.806
S_2	0.028	0.022	0.066
S_3	0.008	0.012	−0.021
Classical DOP	0.859	0.055	0.789
Simplified DOP	0.878	0.039	0.780

camera, Dalsa model 1M150-SA, is able to easily reach the 1-kHz frame rate of the FLC modulator. Unfortunately, it proves far less sensitive than the previous CCD camera. However, since the scene rotates, speckle is less visible than previously. Therefore, we were able to remove the rotating diffuser in order to compensate for the camera's lesser sensitivity.

Figure 10 shows images from movies taken at 35 and 406 Hz. At 35 Hz, the images are only slightly noisy, but at 406 Hz, high-gain systems have been activated, resulting in increased noise. To improve the quality of this method, we can modify the contrast of images by time-consuming numerical postprocessing. In order to work at such high frame rates, however, we must find a technological alternative to this CMOS camera.

4.3 *High-Speed Imaging Polarimeter with a CCD Camera*

In order to get acceptable quality, we replaced the Dalsa CMOS camera with a quite inexpensive analog CCD camera manufactured by Sony. The latter, model XC-HR 57, is much more sensitive than the CMOS camera and can be operated in partial scan mode at up to 240 frames per second without binning. We used the camera at 233 Hz, which

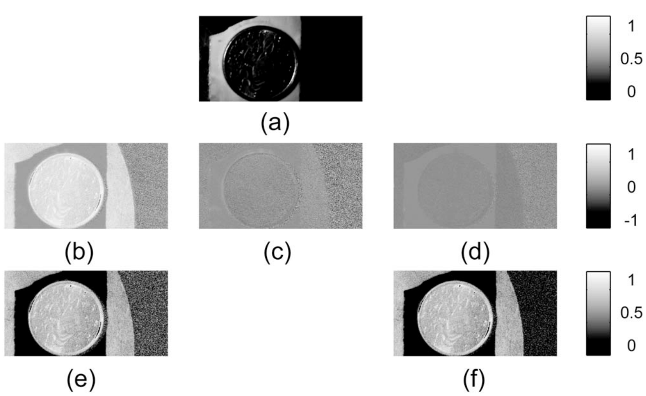

Fig. 9 Stokes images of our dynamic scene obtained with a reference polarizer: (a) S_0, (b) S_1, (c) S_2, (d) S_3 normalized by S_0; (e) the classical DOP according to Eq. (4); (f) the simplified DOP according to Eq. (5).

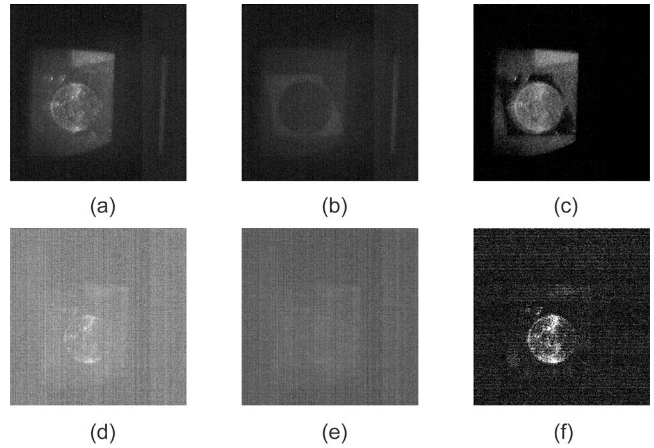

Fig. 10 Images (a) to (c) were acquired with a 35-Hz frame rate; images (d) and (e), with a 406-Hz frame rate. Images (a) and (d) correspond to I_0, images (b) and (e) correspond to I_{90}, and images (c) and (f) depict DOP evaluations.

results in 640×82 images. In order to get high-quality images, the rotating diffuser was put back into the experimental setup.

Figure 11 reports experimental results. This enhanced setup provides quality images in degree of polarization. We can now clearly distinguish the various materials. Nevertheless, a 10- or 12-bit camera would probably greatly increase the SNR of the images.

As far as depolarization properties are concerned, the results are quite similar to those reported in Sec. 3.3. We can particularly notice the strong depolarizing power of the double-sided adhesive tape, which strongly contrasts with the aluminum wheel and the one-euro-cent coin. We can compare the simplified DOP obtained with the rotating quarter-wave plate polarimeter and with the FLC polarimeter (Table 2). These results prove quite similar. We can claim that the FLC polarimeter can correctly estimate the DOP: the differences between results of the two polarimeters may not be significant, since the angular precision in the reference polarimeter is only about 1 deg.

5 Discussion

Results obtained with this implementation prove the point in using a liquid-crystal ferroelectric modulator for high-speed linear DOP evaluation. This implementation can be used to acquire a sequence of DOP pictures describing a dynamic scene containing different materials with various depolarization properties.

This ferroelectric modulator has a maximum frequency of 1 kHz. The only limitation of our implementation is due to the camera's frame rate and to the power of the He-Ne

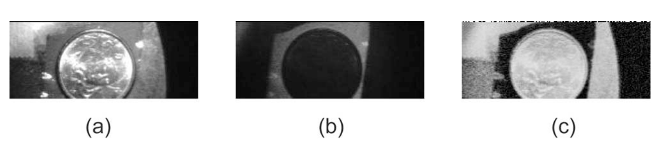

Fig. 11 Images (a) to (c) were acquired at 233 Hz with a CCD camera. Image (a) represents I_0, image (b) represents I_{90}, and image (c) depicts the DOP.

Table 2 Comparison between DOP obtained with the rotating quarter-wave plate polarimeter and with the FLC polarimeter for different elements of our dynamic test scene.

	Simplified DOP		
Measured with	Aluminum wheel	Double-sided adhesive tape	Euro cent coin
Rotating quarter-wave plate	0.878	0.039	0.780
FLC	0.839	0.090	0.749

laser source. A faster sensitive CCD camera can be used, as well as a CMOS camera with hardware postprocessing for image homogenization.

6 Conclusion

We implemented a high-speed imaging polarimeter using a ferroelectric liquid crystal light modulator. Our setup restricts us to the estimation of the degree of polarization. This setup is able to capture moving scenes, providing good-quality images. With an analog CCD camera, we were able to capture images with a quality similar to that provided by mechanically rotating elements. This system can be operated at up to 233 Hz, much faster than other systems using rotating elements or nematic-liquid-crystal modulators. With a faster CMOS camera, images have been captured at 406 Hz, but at the expense of reduced quality, since our CMOS camera is far less sensitive than the CCD camera.

References

1. J. M. Bueno and P. Artal, "Double-pass imaging polarimetry in the human eye," *Opt. Lett.* **24**, 64–66 (1999).
2. B. Laude-Boulesteix, A. de Martino, B. Drévillon, and L. Schwartz, "Mueller polarimetric imaging system with liquid crystals," *Appl. Opt.* **43**, 2824–2832 (2004).
3. P.-Y. Gerligand, R. A. Chipman, E. A. Sornsin, and M. H. Smith, "Polarization signatures of spherical and conical targets measured by Mueller matrix imaging polarimetry," in *Polarization: Measurement, Analysis, and Remote Sensing*, D. H. Goldstein and R. A. Chipman, Eds., pp. 63–73, SPIE (1997).
4. B. J. Deboo, J. M. Sasian, and R. A. Chipman, "Depolarization of diffusely reflecting man-made objects," *Appl. Opt.* **44**, 5434–5445 (2005).
5. G. D. Lewis, D. L. Jordan, and P. J. Roberts, "Backscattering target detection in a turbid medium by polarization discrimination," *Appl. Opt.* **38**, 3937–3944 (1999).
6. M. Floc'h, G. Le Brun, J. Cariou, and J. Lotrian, "Experimental characterization of immersed targets by polar decomposition of the Mueller matrices," *Eur. Phys. J.: Appl. Phys.* **3**, 349–358 (1998).
7. G. W. Kattawar and M. J. Rakovic, "Virtues of Mueller matrix imaging for underwater target detection," *Appl. Opt.* **38**, 6431–6438 (1999).
8. M. Alouini, D. Dolfi, F. Goudail, and P. Réfrégier, "Detection enhancement of low contrast targets through active multispectral polarimetric imaging," in *EOS Topical Meeting on Advanced Imaging Techniques*, pp. 10–12 (2003).
9. L. B. Wolff, T. A. Mancini, P. Pouliquen, and A. G. Andreou, "Liquid crystal polarization camera," *IEEE Trans. Rob. Autom.* **13**, 195–203 (1997).
10. R. A. Chipman, "Depolarization index and the average degree of polarization," *Appl. Opt.* **44**, 2490–2495 (2005).
11. M. W. Williams, "Depolarization and cross polarization in ellipsometry of rough surfaces," *Appl. Opt.* **25**, 3616–3622 (1986).
12. B. Deboo, J. Sasian, and R. Chipman, "Degree of polarization surfaces and maps for analysis of depolarization," *Opt. Express* **12**, 4941 (2004).
13. D. Goldstein, *Polarized Light*, Marcel Dekker, New York, Basel (2003).
14. M. Alouini, F. Goudail, P. Réfrégier, A. Grisard, E. Lallier, and D. Dolfi, "Multispectral polarimetric imaging with coherent illumination: towards higher image contrast," in *Polarization: Measurement, Analysis, and Remote Sensing VI*, D. H. Goldstein and D. B. Chenault, Eds., pp. 133–144, SPIE (2004).
15. S. G. Demos and R. R. Alfano, "Optical polarization imaging," *Appl. Opt.* **36**, 150–155 (1997).
16. J. Cariou, B. Le Jeune, J. Lotrian, and Y. Guern, "Polarization effects of seawater and underwater targets," *Appl. Opt.* **29**, 1689–1695 (1990).
17. E. Hecht, *Optics*, Addison-Wesley, Reading, MA (2002).
18. P. Réfrégier, F. Goudail, and N. Roux, "Estimation of the degree of polarization in active coherent imagery by using the natural representation," *J. Opt. Soc. Am. A* **21**, 2292–2300 (2004).
19. F. Goudail and P. Réfrégier, "Target segmentation in active polarimetric images by use of statistical active contours," *Appl. Opt.* **41**, 874–883 (2002).
20. P. Clémenceau, A. Dogariu, and J. Stryewski, "Polarization active imaging," in *Laser Radar Technology and Applications V*, G. W. Kamerman, U. N. Singh, C. Werner, and V. V. Molebny, Eds., pp. 401–409, SPIE, Orlando, FL (2000).
21. P. Terrier and V. Devlaminck, "Robust and accurate estimate of the orientation of partially polarized light from a camera sensor," *Appl. Opt.* **40**, 5233–5239 (2001).
22. A. M. Gandorfer, "Ferroelectric retarders as an alternative to piezoelastic modulators for use in solar Stokes vector polarimetry," *Opt. Eng.* **38**, 1402–1408 (1999).
23. Y. Hanaoka, "Ferroelectric liquid crystal polarimeter for high-cadence Hα imaging polarimetry," *Sol. Phys.* **222**, 265–278 (2004).
24. K. A. Bauchert and S. A. Serati, "High-speed multi-level 512×512 spatial light modulator," in *Optical Pattern Recognition XI*, D. P. Casasent and T.-H. Chao, Eds., pp. 59–65, SPIE, Orlando, FL (2000).
25. S. A. Serati, G. D. Sharp, R. A. Serati, D. J. McKnight, and J. E. Stockley, "128×128 analog liquid crystal spatial light modulator," in *Optical Pattern Recognition VI*, D. P. Casasent and T.-H. Chao, Eds., pp. 378–387, SPIE, Orlando, FL (1995).
26. K. A. Bauchert, S. A. Serati, and A. Furman, "Advances in liquid crystal spatial light modulators," in *Optical Pattern Recognition XIII*, D. P. Casasent and T.-H. Chao, Eds., pp. 35–43, SPIE (2002).
27. Boulder Nonlinear Systems, "Liquid crystal spatial light modulator: 512×512 multi-level/analog" (2002).
28. L. Bigué, L. Jourdainne, and P. Ambs, "High speed ferroelectric gray-scale spatial light modulator for implementing diffractive optical elements," in *Diffractive Optics and Micro-Optics*, R. Magnusson, Ed., pp. 58–62, OSA, Tucson, AZ (2002).

Albéric Jaulin obtained his engineering degree and postgraduate degree at ESSAIM (College of Computer and Control Engineering, Mulhouse, France), Université de Haute Alsace (UHA). He is currently completing a PhD in optical, electrical, and computer engineering at UHA. He is a member of SFO (Société Française d″Optique) and EOS (European Optical Society).

Laurent Bigué received his engineering degree at the ENSPS (French College of Physics, Strasbourg, France) as well as his postgraduate degree in photonics and microelectronics at the Université Louis Pasteur, Strasbourg, in 1992. He obtained a PhD in optical, electrical, and computer engineering at the Université de Haute Alsace in 1996. He was appointed an assistant professor at ENSISA (College of Engineering of Université de Haute Alsace, Mulhouse, France) in 1998 and has been a professor at ENSISA since 2005. His major interests include optical signal processing, polarimetry, and optical metrology. He is a member of SFO, EOS, and SPIE.

Pierre Ambs is a professor of electrical engineering at the Université de Haute Alsace (Mulhouse, France). His research interests include optical and computer-generated diffractive optical elements, optical pattern recognition, spatial light modulators, and their applications to information optics. Dr. Ambs received his MS (1979), PhD (1982), and Doctorat d'Etat (1987) from the Université de Haute Alsace. He is a member of SPIE, the OSA, the European Optical Society, and the Société Française d'Optique.